Published in final edited form as:

Curr Biol. 2015 November 2; 25(21): 2785–2794. doi:10.1016/j.cub.2015.09.037.

Multiple phylogenetically distinct events shaped the evolution of limb skeletal morphologies associated with bipedalism in the jerboas

Talia Y. Moore[1], **Chris L. Organ**[2], **Scott V. Edwards**[1], **Andrew A. Biewener**[1], **Clifford J. Tabin**[3], **Farish A. Jenkins Jr.**[1], and **Kimberly L. Cooper**[4]

[1]Department of Organismic & Evolutionary Biology, Harvard University, 26 Oxford Street, Cambridge, MA 02138 USA

[2]Montana State University, Department of Earth Sciences, 226 Traphagen Hall, Bozeman, MT 59717 USA

[3]Department of Genetics, Harvard Medical School, 77 Ave Louis Pasteur, Boston, MA 02115 USA

[4]Division of Biological Sciences, University of California San Diego, 9500 Gilman Drive, La Jolla, CA 92093 USA

SUMMARY

Recent rapid advances in experimental biology have expanded the opportunity for interdisciplinary investigations of the evolution of form and function in non-traditional model species. However, historical divisions of philosophy and methodology between evolutionary/organismal biologists and developmental geneticists often preclude an effective merging of disciplines. In an effort to overcome these divisions, we take advantage of the extraordinary morphological diversity of the rodent superfamily Dipodoidea, including the bipedal jerboas, to experimentally study the developmental mechanisms and biomechanical performance of a remarkably divergent limb structure. Here, we place multiple limb character states in a locomotor and phylogenetic context. While obligate bipedalism arose once in the ancestor of extant jerboas, we find that digit loss, metatarsal fusion, between limb proportions, and within hindlimb proportions all evolved independently of one another. Digit loss occurred three times through at least two distinct developmental mechanisms, and elongation of the hindlimb relative to the forelimb is not simply due to growth mechanisms that change proportions within the hindlimb. Furthermore, we find strong evidence for punctuated evolution of allometric scaling of hindlimb elements during the radiation of Dipodoidea. Our work demonstrates the value of leveraging the evolutionary history of a clade to establish criteria for identifying the developmental genetic mechanisms of morphological diversification.

Corresponding author: Kimberly L. Cooper, UC San Diego, 9500 Gilman Drive; MC-0380, La Jolla, CA 92093, (858) 534-1040, kcooper@ucsd.edu.

INTRODUCTION

The vertebrate limb has long been of interest to evolutionary biologists due to the extraordinary diversity of forms, to biomechanists for the corresponding variety of locomotor functions, and to developmental biologists as a model of patterning and morphogenesis. We stand to gain a more complete understanding of the mechanisms that shape the development and evolution of form and function by integrating these traditionally distinct disciplines. We focus on the rodent superfamily, Dipodoidea, comprised of 51 extant species including the quadrupedal birch mice, facultative bipedal jumping mice, and 33 species of obligate bipedal jerboas [1]. Together, these species exhibit diverse limb morphologies with varying degrees of specialization. The most basal species exhibit an ancestral generalized quadrupedal rodent morphology while the most derived bipedal species have lost the pre- and postaxial hindlimb digits, greatly elongated the hindlimbs, and disproportionately elongated and fused the three central metatarsals.

Studies of jerboa anatomy have been largely limited to dissections of a few species and casual observations of captive individuals prior to the 1940s [2–5]. Even at that time, the morphological characters associated with bipedal saltation in the jerboas were noted as similar to those associated with cursorial locomotion in more familiar and better-studied quadrupedal ungulates. Elongated limbs increase range of motion while reduced distal elements decrease the energy required to swing the limb during sustained running [3, 6]. However, the inaccurate and often contorted posture of jerboas in museum exhibits and texts dating to the late 19th and early 20th century [7] highlights a general unfamiliarity in the West with the way these animals actually move.

The diverse morphologies of extant dipodoid rodents have long been a challenge to pre-molecular taxonomists. These trees are well-reviewed elsewhere [1]. Recently, DNA sequence phylogenetics has resolved the relationships of taxa within Dipodoidea, the monophyletic origin of bipedalism, and the subsequent radiation of species [1, 8–10]. Given that the genes included in these analyses are not under selection for bipedal locomotion, these broadly consistent molecular phylogenies likely represent the true taxonomic relationships. Therefore many of the morphological characters previously used to assign relationships are convergent. The consensus molecular tree thus provides an opportunity to understand evolutionary patterns of these complex morphologies.

Here, we first generate posturally-accurate skeletal reconstructions to understand the locomotor advantage of derived skeletal characters of the obligate bipedal jerboa compared to a close quadrupedal relative. We next identify eight distinct hindlimb morphotypes represented within Dipodoidea based on digit number, the extent of metatarsal fusion, and limb element allometry. We then trace the evolutionary history of each character in the context of a multi-locus, time-calibrated molecular phylogeny. We show that the adaptation of limb structure for a specialized locomotor strategy occurred through a combination of temporally and therefore genetically distinct changes during the radiation of Dipodoidea. Our work demonstrates the value of phylogenetic analyses in evolution and development, particularly in species too distantly related for genetic hybridization, in which multiple

intersecting lines of evidence are critical to strengthen hypotheses regarding developmental mechanism that are often initially correlative in nature.

RESULTS

The acquisition of bipedality in jerboas coincides with multiple skeletal transformations [4, 5] that are most informative in the context of a living animal in movement. Thus we generated to-scale postural reconstructions of the complete skeletons of the three-toed lesser Egyptian jerboa, *Jaculus jaculus* and one of the most closely related extant quadrupeds, the Northern birch mouse, *Sicista betulina* [1]. The illustration of *J. jaculus* is informed by X-ray fluoroscopy of a live jerboa (Movie S1A) and is represented in an aerial phase just prior to landing. Since a living birch mouse was not available for imaging, we reconstructed the skeleton of *S. betulina* based on postural data of a morphologically similar semi-arboreal species [11] - the forest deer mouse, *Peromyscus maniculatus* (Movie S1B). While largely qualitative in nature due to specimen limitations, our observations provide context for the major postural and skeletal changes in the evolution of jerboa bipedalism.

Axial skeleton

The foreshortened skull and thorax of *J. jaculus* are suspended from the pelvis by a vertebral column that is highly modified when compared to quadrupedal rodents [5] (Figure 1A). The jerboa vertebral column appears to have a more extreme sigmoidal curvature: the lumbar column of *J. jaculus* aligns almost horizontally with respect to gravity, while the thoracic column dives vertically and curves again with the pronounced dorsiflexion of a shortened neck.

While the first cervical vertebra (C1, or atlas) is freely mobile in the jerboa, the central cervicals (C2–C6), including the axis, are fused ventrally into a single plate and dorsally into a single large spinous process with lateral openings for the egression of the cervical spinal nerves. The posterior cervical vertebra, C7, is unfused. This is concordant with Howell [4] for the genus *Jaculus*, whereas Beddard [12] and Lull [3] reported the posterior six to be fused in *Dipus*. Flower and Lydekker [2] reported all the cervical vertebrae in *Dipus*, *Alactaga* [sic], and *Platycercomys* (now *Pygeretmus*) to be “more or less ankylosed.” Indeed our investigation of several available related taxa (Table S1) indicates varying degrees of fusion with a subset of vertebrae fully fused, as in *J. jaculus*, or tightly articulated with thin fissures between vertebrae as in *Salpingotus thomasi* and *Allactaga tetradactyla*. In *Sicista* there are seven unfused cervical vertebrae, and only C2, the axis, has a prominent neural spine.

As with most rodents [13], *S. betulina* has 13 thoracic vertebrae, and T10 is the anticlinal vertebra. In contrast, there are 12 thoracic vertebrae in *J. jaculus*, and T12 is the anticlinal vertebra. The presence of seven lumbar vertebrae in *J. jaculus* compared to six in *S. betulina* suggests a transformation of T13 into a lumbar vertebra with an additional posterior shift in the position of the anticlinal vertebra. Howell [4] suggested that by transforming the last thoracic vertebra into an additional lumbar vertebra, the jerboa shortens the thorax without decreasing the size of each individual thoracic vertebral element, which we confirmed (Table S2).

Of the four sacral vertebrae in *J. jaculus*, only the first is fused to the ilium whereas the first two are fused in *S. betulina*. Decreased fusion may increase iliosacral mobility during jumping in *J. jaculus* as in frogs that have limited iliosacral contact [14]. The sacrum of *J. jaculus* is widened in comparison to *S. betulina*, and the spinous processes of the lumbar vertebrae are enlarged, which may support greater back musculature and also increase jumping ability [5]. Additionally, the spinous process of the 4th sacral vertebra is enlarged, indicating robust tail suspensory musculature. *J. jaculus* has 24 elongate caudal vertebrae, and the tail is approximately 1.47 times the naso-anal distance (n=3, s.d.=0.12). *S. betulina* has 34 caudal vertebrae, and the tail is 1.25–1.5 times the naso-anal distance varying by population [15, 16].

Appendicular skeleton

The composite hindlimb length from the greater trochanter of the femur to the distal tip of the central metatarsal is approximately 3.2 times the length of the analogous forelimb elements for the jerboa, compared to 1.4 times for the birch mouse (Table S1). Within hindlimb proportions also differ between species. Whereas the femur of *S. betulina* comprises 34.6% and the third metatarsal is 20.5% of total limb length, the femur of *J. jaculus* is 28.6% and the third metatarsal is 30.6% of hindlimb length. The proportion of the tibia is more similar at 44.9% for *S. betulina* and 43.0% for *J. jaculus.* The small vestiges of the first and fifth metatarsals of the jerboa are tucked along the ventral-lateral edges of the fused central canon bone, which is comprised of metatarsals II–IV. The distal-most aspect of the canon bone remains unfused and articulates with each of the three toes. Lastly, the quadrupedal rodents are plantigrade (fore) and digitigrade (hind) (Movie S1B) while the bipedal *J. jaculus* is sub-unguligrade (Movie S1A). The nails and distal toe pads contact the ground while the digits are elevated atop a tuft of coarse bristles on the plantar surface of the toes.

Center of mass

The reduction of the thorax and expansion of the lumbar region together with the position of the body with respect to the limbs in our X-ray videos led us to hypothesize that the center of mass may be shifted in the bipedal jerboa relative to quadrupedal rodents. We found the center of mass of *P. maniculatus* is located approximately 54.5% (n=3; s.d.=0.073%) of the naso-anal distance consistent with the quadrupedal Siberian chipmunk, *Tamias sibiricus* [17]. The center of mass of *J. jaculus* measures only slightly more posterior at 57.5% (n=4; s.d.=0.025%) of the naso-anal distance. More striking, we found in our X-ray videos that the hindlimb base of support of *P. maniculatus* at mid-stance is positioned approximately 74% of the distance from head to tail base while the jerboa hindlimb base of support is approximately 47% of body length. This places the center of mass approximately 19% ahead of the hindlimb base of support of *P. maniculatus* and 11% behind the hindlimb base of support of *J. jaculus*.

Identification of limb morphotypes

We classified eight distinct hindlimb morphotypes among the 51 extant species of Dipodoidea based primarily on degree of metatarsal fusion and number of digits [1, 18]

(Table S3) and broadly considering allometric scaling of the hindlimb and principal components clustering discussed in further detail below. These include the quadrupedal birch mouse (Sicistinae), the facultative bipedal jumping mice (Zapodinae), and six morphotypes within the obligate bipedal jerboas (Figure 2).

One distinctive feature of the *S. betulina* hindlimb relative to other dipodoid rodents is the lateral curvature of the tibia (Figure 2A). Curvature of long bones is indicative of predictable off-axis bending forces [19]. In the case of *S. betulina*, tibial long-axis curvature may reflect laterally-directed loading forces during climbing as evidenced by the mediolateral orientation of the femur and undulation of the pelvis during locomotion in *P. maniculatus* (Movie S2B) [20]. In contrast, *J. jaculus* hindlimbs fall directly below the body during locomotion (Movie S2A), and the tibia is straighter in each of the obligate bipedal species (Figure 2C–H). The shape of the femoral head also transforms from a rounded knob in *S. betulina* (Figure 2A) to a saddle shape with a femoral neck oriented nearly perpendicular with respect to the bone shaft in the most derived of the jerboas (Figure 2F–H).

Compared to quadrupedal *S. betulina*, the facultative bipedal jumping mice, including *Napaeozapus insignis*, have slightly elongated metatarsals comprising a larger proportion of the hindlimb length discussed in detail below (Figure 2B, 5B). Significant morphological diversity arises in the obligate bipedal jerboas. The three and five-toed pygmy jerboas (Cardiocraniinae - Figure 2C, *Salpingotus thomasi* and Figure 2D, *Cardiocranius paradoxus*, respectively) have individual metatarsals that do not fuse. The long-eared jerboa, *Euchoreutes naso* has five toes with elongated and partially fused metatarsals II–IV (Figure 2E, partial fusion indicated by dashed lines). The Allactaginae are represented by *Allactaga sibirica* (Fig 2G) with a fully fused canon bone comprised of metatarsals II–IV and five toes where the central three are much larger and longer than digits I and V. A single species, *A. tetradactyla* (Figure 2F) has lost the anterior-most digit and retains digits II–V. The Dipodinae, including *Jaculus orientalis* (Figure 2H), are characterized by the same elongate and fused central canon bone but have entirely lost the pre- and postaxial digits and have only digits II–IV remaining. Using the molecular reconstruction of Wu and colleagues [9], with the addition of *Allactaga tetradactyla*, we mapped each of these osteological character states.

Digit loss

Early taxonomies placed the four-toed jerboa, *Allactaga tetradactyla*, within the five-toed jerboas of Allactaginae indicating an independent loss of the first digit within this clade [21]. An alternative hypothesis is that the four-toed jerboa represents an ancestral state to the three-toed morphology and that cranial and dental morphologies are convergent. To test these hypotheses, we examined the position of *A. tetradactyla* and found that the species indeed groups within Allactaginae and most closely with *A. hotsoni*, suggesting a relatively recent and independent loss of the first digit (Figure 3A; Figure S1). Additionally, the three-toed pygmy jerboa, *Salpingotus thomasi*, groups with the five-toed pygmy jerboa, *Cardiocranius paradoxus*, and ancestral to the divergence of Euchoreutinae, Allactaginae, and Dipodinae. This suggests the independent loss of digits occurred at least three times - in *Salpingotus* and in Dipodinae with loss of the pre- and postaxial digits and with loss of the

pre-axial digit in *A. tetradactyla*. However, while pre- and postaxial digits are present in many jerboa species, they are effectively non-functional for locomotion in Euchoreutinae and Allactaginae, as they flank the central canon bone and do not contact the substrate (pers. observation).

Skeletal fusion

The single species within Euchoreutinae, *Euchoreutes naso*, also represents the emergence of partial fusion of the three central metatarsals, and all species of Allactaginae and Dipodinae have completely fused central metatarsals (Figure 3B). Thus metatarsal fusion is monophyletic within the jerboas.

Hindlimb-Forelimb Allometry

Allometric scaling refers to a change in the size of an element relative to another or as a proportion of the whole body. Differences in cranial length and body proportions complicate the use of axial length for body size normalization. Additionally, because the taxa are not independent from one another, the variation in morphological measurements in closely related groups would be less than expected under a Brownian Motion model. Thus, we performed a phylogenetically-weighted Principal Components Analysis (pPCA) to remove the effect of relatedness and body size on our morphological measurements [22]. To better understand the scaling relationships and the dynamics of allometric scaling over evolutionary time, we expanded our analysis to a broad selection of rodents representing diverse forms of locomotion.

We used measurements of the femur, tibia, third metatarsus, and humerus in our analysis. Distal forelimb elements were often not available for measurement in many specimens, but the humerus and metacarpals do scale approximately isometrically for available specimens within Myomorpha (Figure S2A). The first phylogenetically-weighted principal component (pPC1) accounts for 90.9% of the variation in the data, loads approximately equally with all of our morphological measurements (Table S4), and therefore associates with changes due to body size. The remaining principal components (pPCs 2, 3, 4) all describe variation in limb proportions independent of body size. pPC2 loads strongly positively with the metatarsus and negatively with the humerus, and accounts for 86.1% of the remaining morphometric variation in limb proportions. This relationship is illustrated by the repeated appearance of rodents with elongate metatarsals, shortened humerus, and large values of pPC2, and rodents with shorter metatarsals, elongate humerus, and small values of pPC2 (Figure 4A; Table S4).

The hypothesis that limb skeletal structures in the body are predominantly shaped according to their functions predicts that grouping animals with similar limb proportions should also categorize species according to similar locomotor ecomorphs. Since pPCs 2, 3, and 4 each represent changes in limb element proportions independent of body size, we performed a clustering analysis on these principal components (Figure 4B; Figure S2B). We identified up to five distinct clusters that are separated predominantly by values in pPC2 and correspond well to known locomotor ecomorphs from diggers and gliders (longer forelimb) to the most derived of obligate bipedal species (longer hindlimb) [18, 23, 24].

Starting from the lowest values of pPC2, the first group includes the fossorial mole-rat (*Spalax*) and bamboo rat (*Rhizomys*), the semi-fossorial hamsters (*Mesocricetus*) [25], and the gliding spiny tailed squirrel (*Anomalurus*). The second group contains fossorial gophers (*Thomomys* and *Geomys*), and the generalist voles (*Microtus*), spiny mouse (*Acomys*), and rats (*Rattus*). *Rattus exulans* falls within the 95% confidence intervals of both this group and the third group, which contains the semi-aquatic beavers (*Castor*), the generalist house mouse (*Mus*), and the semi-arboreal/generalist deer mice (*Peromyscus*) [26] and semi-arboreal birch mouse (*Sicista*). The fourth group has no overlap with the previous and includes the facultatively bipedal jumping mice (*Napaeozapus* and *Zapus*) and kangaroo rat (*Dipodomys*) and the large obligate bipedal springhare (*Pedetes*). The fifth group exhibits the greatest separation from the previous groups and includes all of the obligate bipedal jerboas.

To quantify the allometric scaling relationships within Dipodoidea, we generated log-transformed plots of the combined length of the hindlimb elements (femur, tibia, and third metatarsal) versus the forelimb elements (humerus, ulna, and third metacarpal) (Figure 5A, C). Log transformation of limb lengths allows us to compare the scaling relationships between groups of animals using a linear regression [27]. For comparison to bipedal species, we chose the “mouse-like” generalist/semi-arboreal quadrupedal rodents in the second and third ecomorph groups described above. These all fall along a line (blue) with a slope of 0.991 indicating that the smallest birch mouse (*S. betulina*) has the same hindlimb to forelimb proportions as the largest rat (*R. exulans*). All of the highly derived bipedal Allactaginae and Dipodinae together form a line (red) with very similar slope of 0.979 but with a positively shifted y-intercept from 0.160 to 0.521 indicating an increased length of the hindlimb relative to forelimb. A phylogenetically controlled ANCOVA test strongly supports two regression lines for different limb ratios between the quadrupedal and most-derived bipedal species (Table S5; p=4E-08). The jumping mice (e.g. *Z. hudsonius*), three- and five-toed pygmy jerboas (*S. thomasi* and *C. paradoxus*) and the long-eared *E. naso* lay between and outside the 95% confidence intervals (grey shading) of the regression lines for quadrupedal and derived bipedal species and are designated as “basal bipeds” (orange).

Within-Hindlimb Allometry

We next sought to test the hypothesis that the allometric scaling between limbs is mechanistically attributed to the change in proportion of elements within the hindlimb. In a log-log plot of metatarsus versus femur, the group two and three ecomorphs, including *S. betulina*, fit a regression line (blue) with a slope of 0.729 (Figure 5B). Again, the most derived bipedal jerboas (Allactaginae and Dipodinae) form a line (red) with a y-intercept shifted upward to 0.151 from −0.002 in quadrupedal species and slope of 0.893 indicating a relative increase of metatarsus:femur ratio. Phylogenetically controlled ANCOVA strongly supports two regression lines (Table S5; p=3E-03) compared with a single regression model. The jumping mice (e.g. *Z. hudsonius*) and pygmy jerboas, *S. thomasi* and *C. paradoxus*, fall between these lines. However, while the pygmy jerboas are between the confidence intervals for between limb proportions (Figure 5A), they lie within the 95% confidence interval (grey shading) of derived bipeds for within hindlimb allometry (Figure 5B). This may be in part due to the majority of more derived bipedal jerboas with larger values of metatarsal and

femur lengths, resulting in a spread of the confidence interval at smaller values. This hypothesis is further supported by the observation that *S. thomasi* and *C. paradoxus* have smaller metatarsal:femur ratios than one would expect given their phylogenetic position among obligate bipeds (Figure 5D). A Bayesian phylogenetic outlier test [28] demonstrates that 94% of the predictive distribution for the metatarsal:femur ratio of obligate bipeds lies above the measured ratios of these two species.

In stark contrast to its low hindlimb:forelimb ratio compared to the most derived bipedal jerboa taxa (Figure 5A), the long-eared jerboa, *Euchoreutes naso*, falls within the 95% confidence interval of the regression for metatarsus:femur (Figure 5B). Indeed, while both ratios follow a trend toward increasing values in more derived species, they do not share the same distribution [Figure 5C, D; Wilcoxon signed-rank test: n=19, sum of ranks (V)=190, p=3.82E-6]. Together these trees suggest the mechanisms that establish the proportion of hind relative to forelimb length are genetically separable from the mechanisms that determine proportions within the hindlimb.

Lastly, we analyzed rates of evolutionary allometric growth versus rates of net speciation (nodes along phylogenetic path lengths) as a test for punctuated evolution where the coefficient of determination (R^2) denotes the percent of character variation explained by punctuated evolution, and the slope of the regression (β) represents the magnitude of the effect of punctuation [29]. A correlation between trait values and net speciation suggests that the trait in question underwent punctuated, rather than gradual, evolution - though not necessarily punctuated equilibrium as originally defined by Eldredge and Gould [30] because of the inability to detect periods of stasis. Although the exact process producing such a pattern is difficult to determine [31], such a test does imply that bursts of morphological change were coupled with speciation [29, 32–35].

We find that the lengths (log) of hindlimb elements are all strongly correlated with net speciation along phylogenetic path lengths (Table S6; metatarsal R^2=0.293, β=0.0519, p=0.006; tibia R^2=0.762, β=0.0669, p=8.45E-9; femur R^2=0.657, β=0.0575, p=6.63E-7) while the lengths (log) of forelimb elements are at most marginally significant (Table S6; metacarpal R^2=0.052, β=0.0191, p=0.12; ulna R^2=0.164, β=0.0307, p=0.05; humerus R^2=0.153, β=0.0333, p=0.04). This suggests that hindlimb length underwent more evolutionary change during speciation rather than gradual Darwinian change over time in all branches.

DISCUSSION

The evolution of bipedal locomotion is associated with dramatic changes in structure and posture. Indeed, Hatt [5] accurately depicts the bipedal rodents, jerboas included, as “so compacted as to be popularly described as looking like potatoes on toothpicks.” *J. jaculus* has transformed to an elevated horizontal body posture, suspended from the pelvis, and has shifted the single position of support to lie ahead of the center of mass. This likely increases stability and may require less energy to prevent forward pitching during bipedal locomotion. Cervical fusion and neck shortening in saltatorial rodents may further stabilize the head during the quick maneuvers and high-acceleration jumps typical of jerboa escape behaviors

[5]. With the neck stabilized, the elongate tail may serve as a more effective counterbalance with the potential to control body orientation during the aerial phase of locomotion as has been proposed for kangaroo rats [36] and lizards [37].

The appendicular skeletal changes are even more pronounced than those of the axial skeleton. The straightness of the tibia and the saddle-shaped femoral head suggest reduced variability in the direction of skeletal loading stresses [19] perhaps due to the restricted range of motion primarily limited to a sagittal plane in the strictly cursorial *J. jaculus*. Also associated with the acquisition of bipedal locomotion, the hindlimbs of jerboas are elongate while the forelimbs, released from the constraints of quadrupedal locomotion, are slightly reduced in size. The strong correlation between degree of hindlimb allometric specialization and speciation events at nodes suggests that one may have driven the other. Therefore punctuated evolution likely represents the mode of radiation of Dipodoidea coincident with the climactic changes in the region at the time of the Himalayan uprising that led to ecological diversification [10].

Hindlimb elongation also coincides with fusion of the three central metatarsals into a single bone in all Allactaginae and Dipodinae, which according to beam theory [38] likely increases metatarsal resistance to bending loads by increasing the second moment of area, thus providing more effective weight support. This may be an important structural adaptation since bipedal saltation increases hindlimb loading in two ways. First, the body weight is entirely supported by both or a single hindlimb, depending on gait. Second, saltatory locomotion necessitates an aerial phase, which increases forces associated with take off and landing [39].

While metatarsal fusion occurred once, digit loss has occurred repeatedly in the evolution of Dipodoidea. Hindlimb elongation increases stride length and is compensated for by digit reduction to decrease the limb moment of inertia [3, 6]. Whereas the Allactaginae retain five hindlimb digits, the axial and postaxial digits are smaller and do not make contact with the ground. It is possible therefore that both digit size reduction and loss provide an energetic advantage by decreasing the distal mass and energy required to propel and redirect the motion of the limb.

Our analysis of characters associated with bipedalism also provides an opportunity to approximate genetic complexity and to identify species, structures, and genetic pathways for further analysis. For example, Klippel-Feil Syndrome [40] and Apert Syndrome [41] are human syndromes that include cervical vertebral fusion suggesting pathways (*GDF6* and *FGFR2* respectively) that may underlie the evolution of vertebral fusion. *J. jaculus* has also transformed a thoracic vertebra into a lumbar vertebra, a classic sign of a shift in the spatial domain of expression of *Hox* genes that establish segmental identity [13]. However, the additional shift in the position of the anticlinal vertebra from T10 to T12 in *J. jaculus* suggests the mechanism may be more complex than, for example, a simple anterior shift in register of one of the *Hox* group 10 paralogues [42, 43]. Continuing down the axial column and into the tail, the reduced number of caudal vertebrae in *J. jaculus* suggests an earlier termination of the somite segmentation clock, the developmental process that iteratively pinches off blocks of tissue that will later form the vertebrae [44]. At the same time the total

length of the *J. jaculus* tail is approximately the same proportion of body length as *S. betulina* indicating that at least a subset of the vertebrae elongate more rapidly or for a longer period of time in skeletal development or initiate as larger somites in the embryo.

Within the limb, the evolutionary history of jerboa phenotypes provides insight into mechanisms of digit formation and skeletal growth. We previously showed that axial and postaxial expansion of cell death carves away the tissue that would give rise to the first and fifth digits in *Dipus sagitta* [45]. It is possible that the convergent loss of the first and fifth digits in the pygmy jerboa, *Salpingotus*, occurs by a similar mechanism of expanded cell death, perhaps even by convergence on the same molecular mechanisms. While the independent loss of the first digit in *Allactaga tetradactyla* suggests there are at least two distinct mechanisms, our character analysis of extant species does not rule out a stepwise loss of digit I followed by V in either of the three-toed clades. Loss of the first digit occurs in a variety of human birth defects [46, 47], mouse mutants [48, 49], and throughout evolutionary history, often as a prelude to the subsequent loss of additional digits [50, 51].

In contrast to the discrete nature of digit loss and metatarsal fusion, skeletal allometry manifests as a continuum of values. Close examination of these allometries in the context of phylogenetic relationships demonstrates that the genetic mechanisms determining inter- and intra-limb proportions are uncoupled in Dipodoidea. Most notably, the obligate bipedal *Euchoreutes naso* exhibits a larger hindlimb:forelimb length ratio than any other jerboa, yet also has one of the smallest metatarsus:femur length ratios. Human congenital skeletal dwarfisms and loss-of-function mutations in mice have identified genes that are required for all long bone growth [52–54], but the mechanisms that deploy these genes at the precise time and levels to generate correct individual bone sizes and proportions largely remain a mystery. The genetic uncoupling we observe here indicates that these mechanisms are complex and may act at the level of global control of size in the anterior versus posterior regions of the body as well as at the level of individual limb skeletal elements.

Not only do we highlight the genetic and regional complexity of skeletal growth control, our finding that hindlimb elements have undergone punctuated evolution also provides an opportunity to apply the same punctuation tests to gene sequences of candidates for growth regulation. Since the genes underlying differences in growth have undergone the same selection as the adult morphologies that result from these developmental differences, we expect the degree of sequence divergence of causative loci to similarly associate with the number of nodes along a path. This finding provides strong justification for the generation of draft genome sequences of species at the tips of a variety of path lengths. Together, this work illustrates the extraordinary value of leveraging *a priori* analyses of evolutionary history to inform subsequent analyses of developmental and genetic mechanisms of evolution.

EXPERIMENTAL PROCEDURES

All work with live *Jaculus jaculus* and *Peromyscus maniculatus* were in accordance with Harvard FAS IACUC protocols. All museum specimens that were included in our character analysis are listed in Table S1.

X-ray fluoroscopy recordings were taken at 1000 frames per second using high speed cameras (Photron 1024) mounted into Siemens Tridoros 150 G-3 C-arms and sampled every other frame. Radiation was set at 5 mA and 60 KVp. Jerboas were restricted to a linear path using a cardboard track. The postural reconstruction of *J. jaculus* is represented in an aerial phase just prior to landing (Movie S1A, Frame 2788). The size and shape of each bone was based on the skeleton of a female *J. jaculus* in the private collection of K.C. (JJ 0001). The postural reconstruction of *Sicista betulina* was derived from a live semi-arboreal forest deer mouse, *P. maniculatus* walking along a thin wooden rod and is represented in mid-stance (Movie S1B, Frame 202). The movie also shows loose PVC tubing that was used to induce locomotor instability for a separate project. The skeletal size and shape reconstruction of *S. betulina* is derived from μCT images of a female *S. betulina* alcohol specimen (MVZ 176617) and a male skeleton (AMNH 206585). Hindlimb morphotype reconstructions are based on specimens listed in Table S1.

Center of mass was measured by placing the euthanized animal on a rigid ruler supported by a scale at each end [17]. The animal was arranged into a physiologically relevant position on the ruler and moved anteriorly or posteriorly until the mass recorded on each scale was equal. The anatomical location of the center point between the two scales corresponded to the location of the center of mass as a percentage of naso-anal distance.

We produced a time-calibrated tree with MrBayes (Figure S1). Sequences of 28 species (23 Dipodoidea, 5 outgroups) were used including the Dipodoid species from the work of Wu and colleagues [9] plus the following sequences obtained from Genbank: *Jaculus orientalis* (JN214562.1), *Pygeretmus pumilio* (JF938718.1, JQ347916.1, JQ347936.1, JQ347894.1, JF938696.1, JF938896.1), and *Stylodipus telum* (JF938723.1, JF938802.1, JQ347920.1, JQ347940.1, JQ347898.1, JF938701.1, JF938901.1). DNA sequences for *A. tetradactyla* were obtained by PCR from leg muscle genomic DNA using previously published [9] primers for A2AB, CNR1, GHR, IRBP, LCAT, BRCA1, vWF, ATP7a, CREM, RAG2, and DMP1 (Accession numbers KT164755, KT164756, KT164757, KT164758, KT164759, KT164760, KT164761, KT164762, KT164763, KT164764). We calibrated nodes using divergence times from Date-a-Clade and Wu et al [55]: the root, Dipodidae, mouse/rat split, Cardiocraniinae, and the Dipodinae/Allactaginae split (Supplemental Text). The MCMC procedure ran for 10,000,000 iterations in four chains over two runs, and sampled every 1,000th iteration. The genus *Jaculus* was poorly resolved (*J. blanfordi* and *J. orientalis* were grouped with a posterior probability of 59%) but was used for the comparative analysis as this level of phylogenetic uncertainty has little impact on our results. After the tree was inferred *Allactaga balikunica* was placed manually [56] because no sequences were available.

The resulting tree was embedded into a Rodentia phylogeny [57]. We then trimmed away all taxa except for those associated with morphological data. This tree was used for pPCA and contains 42 taxa: 19 Dipodoidea, 14 Muroidea, and 9 other rodents. Genetic information was available for *Salpingotus koslovi,* but specimens were only available for *S. thomasi. S. thomasi* is therefore listed on the figures at the phylogenetic position of *S. koslovi* since this clade is well-resolved at the genus level. Similarly, *Sicista betulina* morphological data is presented in place of *S. tianshanica* on the phylogeny.

Categorical data representing the number of toes on the hindfeet and the degree of metatarsal fusion (none, partial, full) were collected for each taxon. The length of each long bone segment of the forelimb (humerus, ulna, third metacarpal) and hindlimb (femur, tibia, third metatarsal) was measured by digital microcaliper. Humerus, femur, tibia, and third metatarsal data were included in a phylogenetically-weighted Principal Components Analysis using the phyl.pca function in the Phytools package for R. Clustering analysis was performed on these latter components using the kmeans function in the Stats package for R and is represented as the within groups sum of squares by number of clusters extracted (Figure S2B) [58].

We reconstructed ancestral states for digit loss using the function make.simmap in the Phytools package for R and set five digits as the prior state. The directional pattern of metatarsal fusion without reversion in Dipodoidea suggests that fusion evolves as an ordered state. We therefore used the function ancThresh in the Phytools package for R, which assumes that the discrete character is determined by underlying, ordered, and unobservable continuous traits. We constructed the ancestral states of continuous variables (Forelimb:Hindlimb, Femur:Metatarsus, pPC2) using the function contMap in the Phytools package for R. For each character, we ran the function on all taxa in the rodent clade for which we had data but focus our analyses of discrete characters within Dipodoidea as these have not occurred more broadly within rodents.

For the ANCOVA tests, we used dummy variables (and their interactions with the independent variable) to separate different groups from one another. Likelihood ratio tests for the ANCOVA models compare the dummy-variable (two line) model against a simpler single line model (LRT is 2 x the log-likelihood ratio assuming a chi squared distribution and degrees of freedom equal to the difference in parameters of the models). We assessed significance for the regression lines (including the punctuated evolution regression models) with t-scores ($t = \beta_1/SE$) where β_1 is the slope of the regression line and SE is the standard error of the slope with the degrees of freedom equal to n-2. To account for multiple hypothesis testing we adjusted p-values using the Bonferroni-Holm step-down procedure [59].

We used the maximum likelihood method in BayesTraits v2 (http://www.evolution.rdg.ac.uk) to test for punctuated evolution and perform the ANCOVA tests using the chronogram above. Phylogenetic signal (λ) was estimated during these analyses. To test for punctuated evolution, root-to-tip path lengths are regressed onto the number of nodes (net speciation events) along that path [29]. Here we use log-transformed measurements of limb elements instead of path lengths. A positive relationship between path length and the number of nodes suggests punctuated evolution.

Supplementary Material

Refer to Web version on PubMed Central for supplementary material.

Acknowledgments

We are grateful to Laszlo Meszoly for anatomical illustrations and to Dr. James Hanken for support to complete the artwork. Skeletal specimens were generously provided on loan from the American Museum of Natural History (New York, NY), the National Museum of Natural History (Washington, DC), the Museum of Comparative Zoology (Cambridge, MA), the Museum of Vertebrate Zoology (Berkeley, CA), and the Museum of Southwestern Biology (Albuquerque, NM). We thank Dr. Hopi Hoekstra and Evan Kingsley for providing *P. maniculatus*. TYM attended the course "Paleobiological and phylogenetic approaches to macroevolution" held by the NESCent Academy and supported by the National Evolutionary Synthesis Center (NESCent) NSF #EF-0423641. SVE and KLC thank Dr. Joseph Cook and members of the AIM-UP! research network (NSF #DEB-0956129) for valuable discussion.

References

1. Lebedev VS, Bannikova AA, Pagès M, Pisano J, Michaux JR, Shenbrot GI. Molecular phylogeny and systematics of Dipodoidea: a test of morphology-based hypotheses. Zool Scr. 2013; 42:231–249.
2. Flower, WH.; Lydekker, R. An Introduction to the Study of Mammals, Living and Extinct. A. and C. Black; London: 1891.
3. Lull RS. Adaptations to Aquatic, Arboreal, Fossorial and Cursorial Habits in Mammals. IV. Cursorial Adaptations. Am Nat. 1904; 38:1–11.
4. Howell AB. The Saltatorial Rodent Dipodomys: The Functional and Comparative Anatomy of Its Muscular and Osseous Systems. Proc Am Acad Arts Sci. 1932; 67:377–536.
5. Hatt RT. The vertebral columns of ricochetal rodents. Bull Amer Mus Nat Hist. 1932; 63:599–738.
6. Biewener AA. Biomechanical consequences of scaling. J Exp Biol. 2005; 208:1665–1676. [PubMed: 15855398]
7. Jones, TR. General outline of the Organization of the Animal Kingdom, and Manual of Comparative Anatomy. 4. J. Van Voorst; London: 1871.
8. Zhang Q, Xia L, Kimura Y, Shenbrot G, Zhang Z, Ge D, Yang Q. Tracing the Origin and Diversification of Dipodoidea (Order: Rodentia): Evidence from Fossil Record and Molecular Phylogeny. Evol Biol. 2013; 40:32–44.
9. Wu S, et al. The Evolution of Bipedalism in Jerboas (Rodentia: Dipodoidea): Origin in Humid and Forested Environments. Evolution. 2014; 68(7):2108–2118. [PubMed: 24628052]
10. Pisano J, Condamine FL, Lebedev V, Bannikova A, Quere JP, Shenbrot GI, Pages M, Michaux JR. Out of Himalaya: the impact of past Asian environmental changes on the evolutionary and biogeographical history of Dipodoidea (Rodentia). J Biogeogr. 2015; 42:856–870.
11. Horner BE. Arboreal adaptations of Peromyscus with special reference to use of the tail. Contrib Lab Vertebr Biol Univ Mich. 1954; (61):1–84.
12. Beddard, FE. Mammalia (Cambridge Natural History). Vol. X. Macmillan and Co; London: 1902.
13. Burke AC, Nelson CE, Morgan BA, Tabin C. Hox genes and the evolution of vertebrate axial morphology. Development. 1995; 121:333–46. [PubMed: 7768176]
14. Shubin NH, Jenkins FA. An Early Jurassic jumping frog. Nature. 1995; 377:49–52.
15. Shenbrot, GI.; Sokolov, VE.; Heptner, VG. Jerboas: Mammals of Russia and Adjacent Regions. Amerind Publishing; New Dehli: 2008.
16. Olsen, L-H. Tracks and Signs of the Animals and Birds of Britain and Europe. Princeton University Press; 2013.
17. Lammers AR, Zurcher U. Torque around the center of mass: dynamic stability during quadrupedal arboreal locomotion in the Siberian chipmunk (Tamias sibiricus). Zool Jena Ger. 2011; 114:95–103.
18. Walker, EP. Mammals of the world. Baltimore: John Hopkins Press; 1964.
19. Bertram JE, Biewener AA. Bone curvature: sacrificing strength for load predictability? J Theor Biol. 1988; 131:75–92. [PubMed: 3419194]
20. Biewener A. Scaling Body Support in Mammals - Limb Posture and Muscle Mechanics. Science. 1989; 245:45–48. [PubMed: 2740914]

21. Wilson, DE.; Reeder, DM. Mammal Species of the World: A Taxonomic and Geographic Reference. JHU Press; 2005. Superfamily Dipodoidea.
22. Revell LJ. Size-Correction and Principal Components for Interspecific Comparative Studies. Evolution. 2009; 63:3258–3268. [PubMed: 19663993]
23. Samuels JX, Van Valkenburgh B. Skeletal indicators of locomotor adaptations in living and extinct rodents. J Morphol. 2008; 269:1387–1411. [PubMed: 18777567]
24. Feldhamer, GA.; Drickamer, LC.; Vessey, SH.; Merritt, JF.; Krajewski, C. Mammalogy: Adaptation, Diversity, Ecology. JHU Press; 2015.
25. Larimer SC, Fritzsche P, Song Z, Johnston J, Neumann K, Gattermann R, McPhee ME, Johnston RE. Foraging behavior of golden hamsters (Mesocricetus auratus) in the wild. J Ethol. 2010; 29:275–283.
26. Hyams SE, Jayne BC, Cameron GN. Arboreal habitat structure affects locomotor speed and perch choice of white-footed mice (Peromyscus leucopus). J Exp Zool Part Ecol Genet Physiol. 2012; 317:540–551.
27. Huxley JS. Constant differential growth-ratios and their significance. Nature. 1924; 114:895–896.
28. Organ C, Nunn CL, Machanda Z, Wrangham RW. Phylogenetic rate shifts in feeding time during the evolution of Homo. Proc Natl Acad Sci. 2011; 108:14555–14559. [PubMed: 21873223]
29. Pagel M, Venditti C, Meade A. Large punctuational contribution of speciation to evolutionary divergence at the molecular level. Science. 2006; 314:119–121. [PubMed: 17023657]
30. Eldredge, N.; Gould, SJ. Punctuated equilibria: an alternative to phyletic gradualism. Freman, Cooper & Co; USA: 1972.
31. Pennell MW, Harmon LJ, Uyeda JC. Is there room for punctuated equilibrium in macroevolution? Trends Ecol Evol. 2014; 29:23–32. [PubMed: 23978567]
32. Mattila TM, Bokma F. Extant mammal body masses suggest punctuated equilibrium. Proc R Soc B-Biol Sci. 2008; 275:2195–2199.
33. Venditti C, Pagel M. Speciation as an active force in promoting genetic evolution. Trends Ecol Evol. 2010; 25:14–20. [PubMed: 19720426]
34. Rabosky DL, et al. Rates of speciation and morphological evolution are correlated across the largest vertebrate radiation. Nat Commun. 2013; 4:Article number 1958.
35. Venditti C, Pagel M. Plenty of room for punctuational change. Trends Ecol Evol. 2014; 29:71–72. [PubMed: 24388287]
36. Bartholomew GA, Caswell HH. Locomotion in Kangaroo Rats and Its Adaptive Significance. J Mammal. 1951; 32:155–169.
37. Libby T, Moore TY, Chang-Siu E, Li D, Cohen DJ, Jusufi A, Full RJ. Tail-assisted pitch control in lizards, robots and dinosaurs. Nature. 2012; 481:181–184. [PubMed: 22217942]
38. Gere, JM.; Timoshenko, SP. Mechanics of Materials - Fourth SI. Aydin, I., editor. Cheltenham: Nelson Thornes Ltd; 1999.
39. Hayes G, Alexander RM. The hopping gaits of crows (Corvidae) and other bipeds. J Zool. 1983; 200:205–213.
40. Tassabehji M, Fang ZM, Hilton EN, McGaughran J, Zhao Z, de Bock CE, Howard E, Malass M, Donnai D, Diwan A, et al. Mutations in GDF6 are associated with vertebral segmentation defects in Klippel-Feil syndrome. Hum Mutat. 2008; 29:1017–1027. [PubMed: 18425797]
41. Yu K, Herr AB, Waksman G, Ornitz DM. Loss of fibroblast growth factor receptor 2 ligand-binding specificity in Apert syndrome. Proc Natl Acad Sci U S A. 2000; 97:14536–14541. [PubMed: 11121055]
42. Carapuço M, Nóvoa A, Bobola N, Mallo M. Hox genes specify vertebral types in the presomitic mesoderm. Genes Dev. 2005; 19:2116–2121. [PubMed: 16166377]
43. Hostikka SL, Gong J, Carpenter EM. Axial and appendicular skeletal transformations, ligament alterations, and motor neuron loss in Hoxc10 mutants. Int J Biol Sci. 2009; 5:397–410. [PubMed: 19623272]
44. Pourquie O. The segmentation clock: Converting embryonic time into spatial pattern. Science. 2003; 301:328–330. [PubMed: 12869750]

45. Cooper KL, Sears KE, Uygur A, Maier J, Baczkowski KS, Brosnahan M, Antczak D, Skidmore JA, Tabin CJ. Patterning and post-patterning modes of evolutionary digit loss in mammals. Nature. 2014; 511:41–45. [PubMed: 24990742]
46. Basson C, Cowley G, Solomon S, Weissman B, Poznanski A, Traill T, Seidman J, Seidman C. The Clinical and Genetic Spectrum of the Holt-Oram Syndrome (heart-Hand Syndrome). N Engl J Med. 1994; 330:885–891. [PubMed: 8114858]
47. Gold NB, Westgate MN, Holmes LB. Anatomic and etiological classification of congenital limb deficiencies. Am J Med Genet A. 2011; 155:1225–1235. [PubMed: 21557466]
48. Mortlock DP, Post LC, Innis JW. The molecular basis of hypodactyly (Hd): A deletion in Hoxa13 leads to arrest of digital arch formation. Nat Genet. 1996; 13:284–289. [PubMed: 8673126]
49. Bruneau BG, Nemer G, Schmitt JP, Charron F, Robitaille L, Caron S, Conner DA, Gessler M, Nemer M, Seidman CE, et al. A murine model of Holt-Oram syndrome defines roles of the T-box transcription factor Tbx5 in cardiogenesis and disease. Cell. 2001; 106:709–721. [PubMed: 11572777]
50. Shapiro M. Developmental morphology of limb reduction inhemiergis (squamata: scincidae): chondrogenesis, osteogenesis, and heterochrony. J Morphol. 2002; 254:211–231. [PubMed: 12386893]
51. Prothero, DR.; Foss, SE. The Evolution of Artiodactyls. JHU Press; 2007.
52. Deng CX, WynshawBoris A, Zhou F, Kuo A, Leder P. Fibroblast growth factor receptor 3 is a negative regulator of bone growth. Cell. 1996; 84:911–921. [PubMed: 8601314]
53. Chusho H, Tamura N, Ogawa Y, Yasoda A, Suda M, Miyazawa T, Nakamura K, Nakao K, Kurihara T, Komatsu Y, et al. Dwarfism and early death in mice lacking C-type natriuretic peptide. Proc Natl Acad Sci U S A. 2001; 98:4016–4021. [PubMed: 11259675]
54. Minina E, Kreschel C, Naski MC, Ornitz DM, Vortkamp A. Interaction of FGF, lhh/Pthlh, and BMP signaling integrates chondrocyte proliferation and hypertrophic differentiation. Dev Cell. 2002; 3:439–449. [PubMed: 12361605]
55. Wu S, Wu W, Zhang F, Ye J, Ni X, Sun J, Edwards SV, Meng J, Organ CL. Molecular and Paleontological Evidence for a Post-Cretaceous Origin of Rodents. PLoS ONE. 2012; 7:e46445. [PubMed: 23071573]
56. Smith, AT.; Xie, Y.; Hoffmann, RS.; Lunde, D.; MacKinnon, J.; Wilson, DE.; Wozencraft, WC. A Guide to the Mammals of China. Princeton University Press; 2010.
57. Fabre PH, Hautier L, Dimitrov D, Douzery EJP. A glimpse on the pattern of rodent diversification: a phylogenetic approach. Bmc Evol Biol. 2012; 12:88. [PubMed: 22697210]
58. Hothorn, T.; Everitt, BS. A Handbook of Statistical Analyses using R. 3. CRC Press; 2014.
59. Holm S. A Simple Sequentially Rejective Multiple Test Procedure. Scand J Stat. 1979; 6:65–70.

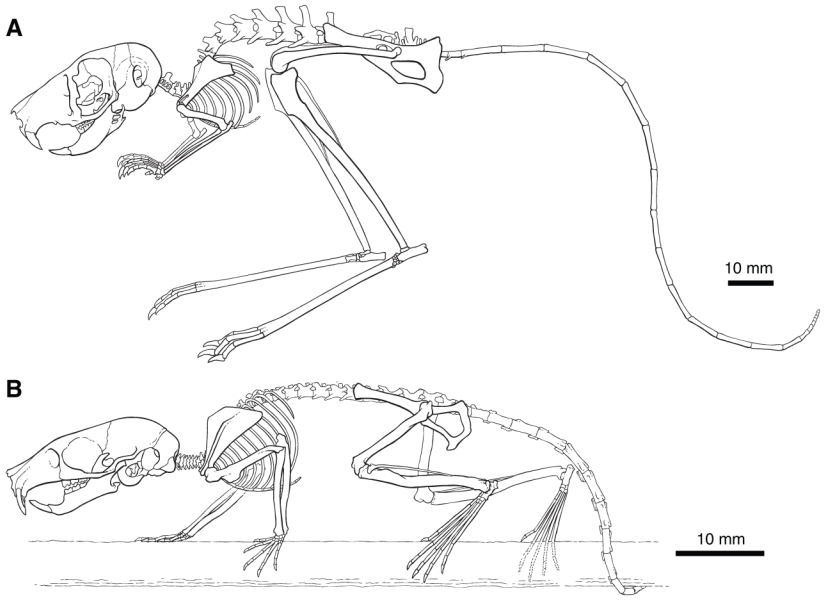

Figure 1.
Comparison of the bipedal lesser Egyptian jerboa (A, *Jaculus jaculus*) and the semi-arboreal quadrupedal Northern birch mouse (B, *Sicista betulina*) in the context of posture in movement.

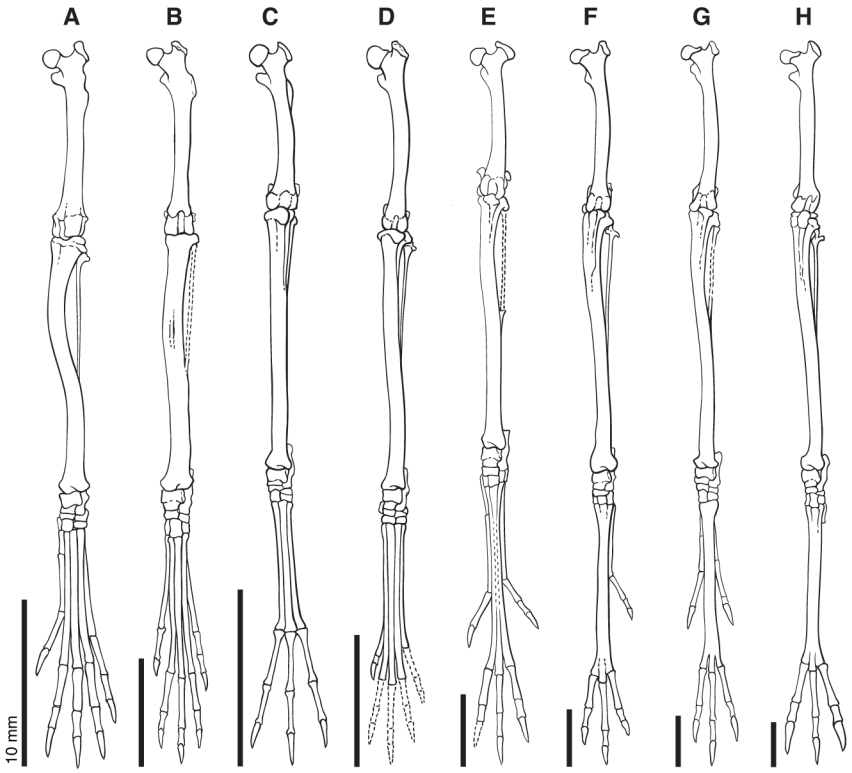

Figure 2. Frontal illustrations of the hindlimbs of a representative of each morphotype scaled to the same length

(A) *Sicista betulina*. (B) *Napaeozapus insignis insignis*. (C) *Salpingotus thomasi*. (D) *Cardiocranius paradoxus*. (E) *Euchoreutes naso*. (F) *Allactaga tetradactyla*. (G) *Allactaga sibirica* [*mongolica*]. (H) *Jaculus orientalis*. Dashed outlines indicate missing elements.

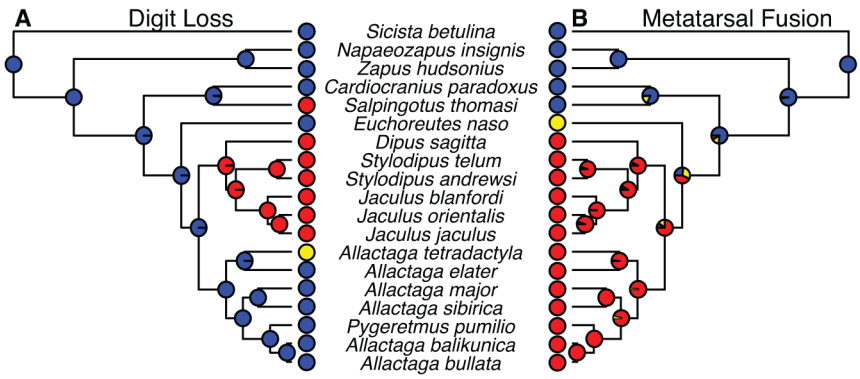

Figure 3. Discrete characters, (A) digit loss and (B) metatarsal fusion, mapped on a molecular phylogeny of Dipodoidea

The ancestral state is blue, the intermediate derived state is yellow (four toes or partially fused), and the ultimate derived state is red. The probability of the ancestor at each node taking a specific state is denoted by a pie graph at that node.

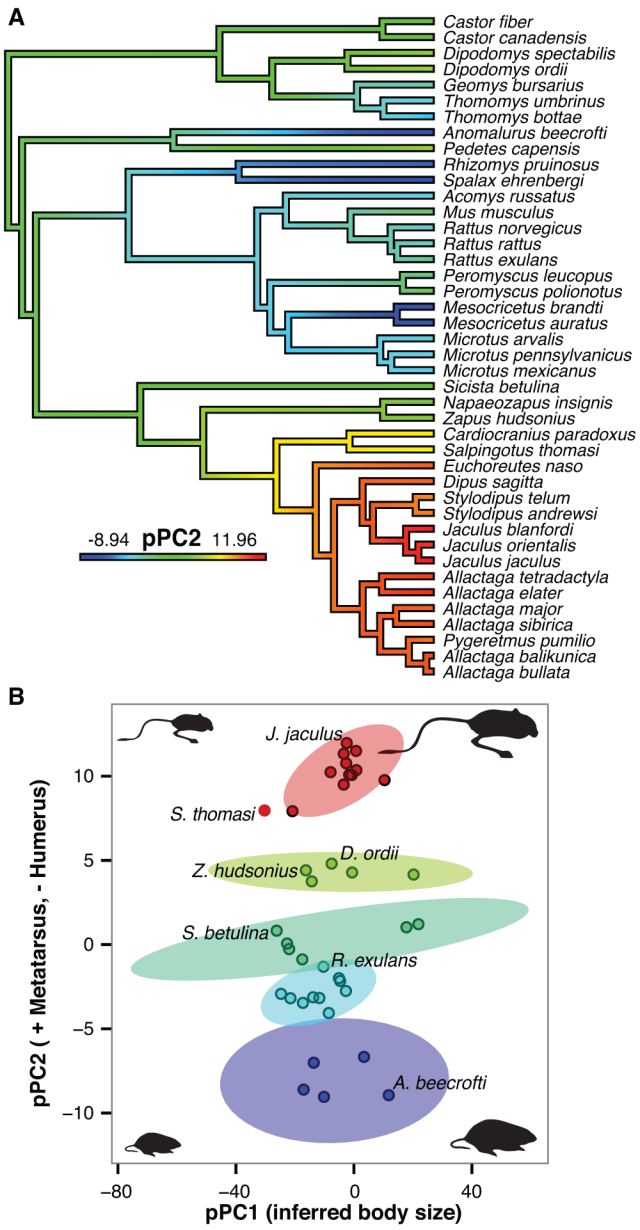

Figure 4. Phylogenetically corrected principal components analysis illustrates major proportional differences across rodent limbs

(A) pPC2 is mapped as a continuous trait on the phylogeny of rodents with ancestral states reconstructed (graded color). (B) Clusters of similar ecomorphs plotted with respect to pPC1 (representing variation due to body size; 90.9% of the total variance) and pPC2 (representing degree and direction of limb specialization; 86.1% of remaining variance with pPC1 removed). Shaded ellipses demark the 95% confidence interval of each cluster.

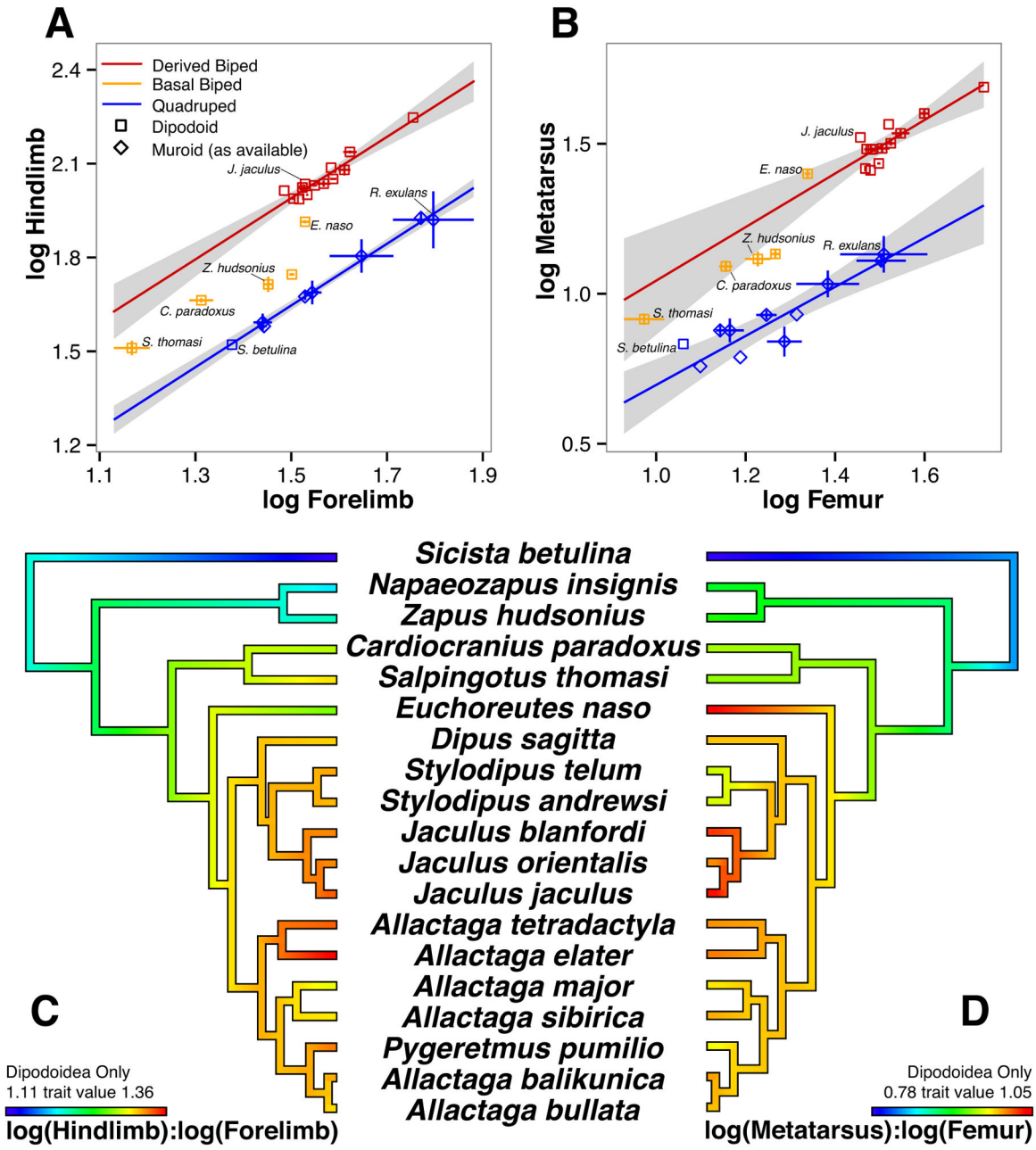

Figure 5. Allometric scaling between limbs and within the hindlimb illustrates the complex evolution of proportion

Log-log plots illustrating scaling of (A) hindlimb versus forelimb and (B) metatarsus versus femur. Derived bipeds, Allagtaginae and Dipodinae, are designated red. Basal and intermediate bipeds, Zapodinae, Cardiocraniinae, and Euchoreutinae, are designated orange. Quadrupeds that cluster together in the second and third ecomorph groups are designated blue. Grey shading indicates 95% confidence intervals, and vertical and horizontal lines represent variation one standard deviation away from the mean. Phylogenies of Dipodidae,

with (C) $\log_{10}$(hindlimb):$\log_{10}$(forelimb) or (D) $\log_{10}$(metatarsal):$\log_{10}$(femur) mapped as continuous traits with ancestral states reconstructed by maximum likelihood (graded color).